bioRxiv preprint doi: https://doi.org/10.1101/2022.12.08.519675; this version posted December 9, 2022. The copyright holder for this preprint (which was not certified by peer review) is the author/funder, who has granted bioRxiv a license to display the preprint in perpetuity. It is made available under aCC-BY 4.0 International license.

Spontaneous activation of cortical somatosensory networks depresses their excitability in preterm human neonates

Kimberley Whitehead [1], Mohammed Rupawala [1], Maria Pureza Laudiano-Dray [1], Judith Meek [2], Sofia Olhede [3], Lorenzo Fabrizi [1]

[1] Department of Neuroscience, Physiology and Pharmacology, University College London, London, United Kingdom
[2] Elizabeth Garrett Anderson Obstetric Wing, University College London Hospitals, London, United Kingdom
[3] Department of Mathematics, Ecole Polytechnique Federale de Lausanne, Lausanne, Switzerland

Abstract

Introduction
The activity of the developing cortex is characteristically discontinuous where sudden high amplitude bursts interrupt periods of quiescent background. While the functional importance of this activity is clear, its aetiology is not known. Here, we hypothesise that this alternating pattern arises because of "refractoriness" of cortical networks following spontaneous activation.
Methods
To test this hypothesis, we assessed whether spontaneous activity in sensory networks depressed their excitability by measuring the impact of ongoing activity on the response to an external sensory stimulus. We recorded cortical activity before and after mechanical tactile stimulation of hands and feet in 35 preterm infants of median 32 weeks post-menstrual age.
Results
Mechanical stimulation evoked wideband energy increases with two distinct peaks within the delta and alpha-beta band. The delta activity engaged extended cortical areas, while the faster activity engaged local somatotopically specific areas. By then characterising the spectro-spatial properties of the spontaneous activity preceding stimulation, we showed that baseline energy with a distribution and spectral profile similar to that of somatosensory-evoked activity dampened the energy changes elicited by touching the body.
Discussion
Sensory-evoked activity in preterm human neonates likely represents the coordinated activation of extended (tangential) and local (e.g. columnar) cortical aggregates. The occurrence of spontaneous cortical events in the same cortical regions depresses their excitability preventing their immediate re-engagement. This "refractoriness" offers the first etiological explanation to the cyclical burst-quiescence pattern typical of preterm cortical activity.

Introduction

Organised endogenous activity across the central nervous system is a characterising feature of developing vertebrate neuronal circuits. This activity is necessary for initial development of neuronal ensembles and, in the cortex, engages columnar and extended networks, establishing the template of the mature functional architecture before the arrival of sensory signals (Molnár et al., 2020). This spontaneous activity is characteristically discontinuous where sudden high amplitude bursts of synchronous neuronal activity interrupt periods of quiescent background (Khazipov and Luhmann, 2006). This cyclical pattern can be explained by an excitatory recurrent network that encounters activity-dependent depression (Tabak et al., 2000). Indeed, spontaneous activity transiently depresses synaptic responsiveness to incoming stimuli in embryonic spinal cord preparations ("refractoriness"), possibly because of transmitter depletion and ligand-induced changes in postsynaptic currents, which

bioRxiv preprint doi: https://doi.org/10.1101/2022.12.08.519675; this version posted December 9, 2022. The copyright holder for this preprint (which was not certified by peer review) is the author/funder, who has granted bioRxiv a license to display the preprint in perpetuity. It is made available under aCC-BY 4.0 International license.

slowly recovers in the inter-burst interval (Fedirchuk et al., 1999). This refractory period is related to after-hyperpolarization of amacrine cells (Zheng et al., 2006) which plays a key role in defining the propagation domains of spontaneous retinal waves (Feller et al., 1996; Godfrey and Swindale, 2007) and also occurs in spinal neurons (O'Donovan, 1999). The episodic nature of activity bouts is thought to provide a high signal-to-noise ratio to the circuit, which could enhance synaptic efficacy in developing networks (O'Donovan, 1999; Tiriac et al., 2014).

Early cortical activity in humans is also highly discontinuous. The preterm electroencephalograph (EEG) is characterised by high voltage transient events (delta brushes and temporal theta) separated by low amplitude inter-burst intervals until about 35 weeks (Wallois et al., 2021). These spontaneous activity bursts occur with varying topographical configurations (Arichi et al., 2017) which can sometimes resemble those evoked by external stimulation (Bourel-Ponchel et al., 2021; Wallois et al., 2021; Whitehead et al., 2016). The diagnostic and prognostic importance of this characteristic pattern of activity is well established (Guérit et al., 2009; Watanabe et al., 1999; Whitehead et al., 2016), however, its aetiology, i.e. why the preterm EEG is discontinuous, is not known.

Here, we hypothesise that, as in other species, the preterm EEG is highly discontinuous because of "refractoriness" of cortical networks following spontaneous activation. To test this hypothesis, we assessed whether spontaneous activity in sensory networks depressed their excitability by measuring the impact of ongoing activity on the response to an external sensory stimulus.

MATERIAL AND METHODS

Subjects

Thirty-five preterm infants were recruited for this study from the neonatal wards at the Elizabeth Garrett Anderson wing of University College London Hospitals (Table 1). Ethical approval was obtained from the NHS Research Ethics Committee, and informed written parental consent was obtained prior to each study. No neonates were acutely unwell at the time of study, required mechanical ventilation, or were receiving analgesics or anti-seizure medication. Exclusion criteria included a diagnosed chromosomal abnormality, high-grade germinal matrix-intraventricular haemorrhage (GM-IVH: grade III or above), or birth weight below the 2nd centile. All EEGs were assessed as normal for postmenstrual age by a clinical neurophysiologist (KW) (Tsuchida et al., 2013).

EEG recording set-up

Up to nineteen recording electrodes (disposable Ag/AgCl cup electrodes) were positioned according to the modified international 10/10 electrode placement system at F3, F4, FCz, Cz, CPz, C3, C4, CP3, CP4, F7, F8, T7, T8, P7, P8, TP9, TP10, O1 and O2. A reduced number of electrodes were applied if the infant became unsettled during set-up (median 18; range 11-19). The reference electrode was placed at Fz and the ground electrode was placed at FC5/6. Target impedance of electrodes was <10 kΩ (André et al., 2010). A single lead I ECG was recorded from both shoulders. Respiratory movement was monitored with an abdominal movement transducer. EEG was recorded with a direct current (DC)-coupled amplifier from DC-800Hz using a Neuroscan (Scan 4.3) SynAmps2 EEG/EP recording system. Signals were digitized with a sampling rate of 2 kHz and a resolution of 24 bit.

Sensory stimulation

Tactile stimuli were delivered by tapping the infants' hands and feet while naturally asleep in the cot or held by their parents, with a hand-held tendon hammer (Supplementary Video 1). The hammer had a piezo-electric transducer that allowed to measure the force applied at each tap, and to record the precise timing of the stimulation on the EEG recording (Worley et al., 2012). A train of somatosensory stimuli was delivered to each limb. The interstimulus interval was large, variable, and self-paced by

bioRxiv preprint doi: https://doi.org/10.1101/2022.12.08.519675; this version posted December 9, 2022. The copyright holder for this preprint (which was not certified by peer review) is the author/funder, who has granted bioRxiv a license to display the preprint in perpetuity. It is made available under aCC-BY 4.0 International license.

the experimenter (average 8–20 s). In case the infant moved, the tap was delayed by several seconds to avoid potential modulation of the somatosensory response by the movement (Saby et al., 2016) and allow movement artefacts to resolve. The sequence in which the limbs were stimulated varied across subjects. We attempted to stimulate every limb at every test occasion, but this was not always possible for example when a cannula was present, or if the infant became unsettled. This resulted in a total of 101 stimulation trains (i.e. stimulated limbs) of 2-48 taps (mean 15). The sleep state immediately prior to the stimulation train was categorised according to EEG and respiratory criteria: active sleep in 68/101 and quiet sleep in 33/101.

Table 1. Demographics of the sample

	Total
No. of neonates	35
No. of stimulation trains	101 (48 hands, 53 feet)
Median (range) PMA at time of study (weeks+days)	32+6 (28+2-35+5)
Median (range) PNA at study (days)	7 (2-33)
Sex (% female)	40%
Multiple gestation neonates	31%
Median (range) birth weight (g)	1575 (785-2440)

PNA indicates postnatal age; PMA indicates postmenstrual age: gestational age at birth plus PNA; Preterm = <37 weeks

EEG pre-processing

Data pre-processing was carried out using EEGLAB v.13 (Swartz Center for Computational Neuroscience) and custom written MATLAB functions. Continuous EEG data were filtered with a comb filter consisting of notch filters at 50 Hz and its harmonics (100 and 150 Hz) to remove mains noise. Each notch filter was a band-stop 4th order zero-phase shift Butterworth filter with a bandwidth of 4 Hz. Continuous EEG data were then epoched from -3 to + 3 seconds around the stimulus to capture the slowest component of a delta brush event. This led to 804 foot-stimulus epochs and 700 hand-stimulus epochs. Bad channels (poor contact with the scalp) were removed from 13 datasets (median: 1 channel, range: 1-3 channels) and then estimated with spherical interpolation as implemented in EEGLAB. EEG recordings following stimulation of the left hemi-body were 'side-swapped' so that recordings contralateral to the stimulation site appear on the 'same side' of the scalp. There are no differences between somatosensory responses to right vs. left body stimulation in preterm infants (Leikos et al., 2020).

Analysis of stimulus-evoked EEG power changes

We first defined the functional engagement of somatosensory cortical networks as the spectro-spatial characteristics of the EEG power changes elicited by tactile stimulation of hands and feet across the whole scalp. To do that, we compared the median power periodogram (0.2-40 Hz) of the 3-seconds post-stimulus segment to that of the 3-seconds baseline at every channel. Each segment was tapered with the first discrete prolate spheroidal sequence before calculating the individual power periodogram. We then took the median power periodogram across all trials for the baseline ($\hat{S}_B^{(k)}(\omega)$) and post-stimulus ($\hat{S}_S^{(k)}(\omega)$) segments at each electrode k (where ω denotes frequency). To assess whether there was a significant difference between these quantities (i.e. whether there was a

bioRxiv preprint doi: https://doi.org/10.1101/2022.12.08.519675; this version posted December 9, 2022. The copyright holder for this preprint (which was not certified by peer review) is the author/funder, who has granted bioRxiv a license to display the preprint in perpetuity. It is made available under aCC-BY 4.0 International license.

significant change in the median power periodogram following stimulation) we computed the ratio $\hat{T}^{(k)}(\omega) = \hat{S}_S^{(k)}(\omega)/\hat{S}_B^{(k)}(\omega)$ and assessed its significance as previously described (Fabrizi et al., 2016). Significance threshold was set at $\alpha = 0.05$, however, because this test was conducted at any frequency ω of the frequency grid, we used false discovery rates to correct for multiple comparisons. Moreover, we also used Bonferroni correction to account for testing at multiple electrodes (n = 19). We then plotted the scalp distributions of these changes in the slow-delta (0.2-2 Hz), fast-delta (2-4 Hz), theta (4-8), alpha-low beta (8-20 Hz) and high beta-gamma (20-40 Hz) bands on a 3D head mesh for illustration purposes.

Analysis of spontaneous EEG power effect on stimulus-evoked changes

We then wanted to test whether the endogenous activation of somatosensory cortical networks influenced their stimulus-driven recruitment. As we had no control over the ongoing activity at the time of stimulation, we had to assess whether the somatosensory networks happened to be active before each of our stimuli. To do that we compared the spectral and spatial profile of the EEG power preceding each stimulus with that of the median EEG power changes elicited by tactile stimulation (somatosensory-evoked template). A close match between them would imply that the somatosensory cortical networks were spontaneously active before the stimulus. To assess this, we used a multiple linear regression model with interaction of the form:

$$T_i^{tot} = \beta_0 + \beta_1 S_{B,i}^{tot} + \beta_2 sim_i^{tot} + \beta_{12}(S_{B,i}^{tot} * sim_i^{tot}), \quad (1)$$

where T_i^{tot} represents a summary measure of change in EEG power elicited by stimulus i (stimulus response); $S_{B,i}^{tot}$ a summary measure of the ongoing endogenous EEG power preceding the stimulus and sim_i^{tot} the similarity between the EEG power preceding the stimulus and that of the median EEG power changes elicited by tactile stimulation. We now define these quantities.

We first calculated the whole band (0.2-40 Hz) energy content $S_{B\Omega,i}^{(k)}$ and $S_{S\Omega,i}^{(k)}$ preceding and following each stimulus i and the stimulus-related change $T_{\Omega,i}^{(k)} = S_{S\Omega,i}^{(k)}/S_{B\Omega,i}^{(k)}$ at every electrode k, where:

$$S_{B\Omega,i}^{(k)} = \int_{\omega} S_{B,i}^{(k)}(\omega)d\omega \quad (2)$$

and

$$S_{S\Omega,i}^{(k)} = \int_{\omega} S_{S,i}^{(k)}(\omega)d\omega \quad (3)$$

where $S_{B,i}^{(k)}(\omega)$ and $S_{S,i}^{(k)}(\omega)$ are the EEG prediograms preceding and following each stimulus i. T_i^{tot} and $S_{B,i}^{tot}$ were then calculate as the Euclidean norm of these energy vectors in channel space and converted to decibels as:

$$S_{B,i}^{tot} = 10log_{10}\left\|S_{B\Omega,i}^{(k)}\right\|, \quad (4)$$

and

$$T_i^{tot} = 10log_{10}\left\|T_{\Omega,i}^{(k)}\right\|. \quad (5)$$

To calculate sim_i^{tot}, we compared the topographical distribution of the EEG power preceding each stimulus with that of the median EEG power changes elicited by tactile stimulation at five EEG bands j (slow-delta, 0.2-2 Hz; fast-delta, 2-4 Hz; theta, 4-8 Hz; alpha-low beta, 8-20 Hz and high beta-gamma, 20-40 Hz). For each band, we defined the median EEG power change elicited by tactile stimulation (this can be seen as the somatosensory cortical networks activation) as:

$$\hat{T}_j^{(k)} = \frac{\int_{\omega\in j}\hat{S}_S^{(k)}(\omega)d\omega}{\int_{\omega\in j}\hat{S}_B^{(k)}(\omega)d\omega}, \quad (6)$$

and the EEG power preceding each stimulus as:

$$S_{B,ij}^{(k)} = \int_{\omega\in j} S_{B,i}^{(k)}(\omega)d\omega. \quad (7)$$

We then calculated the cosine similarity between the topographies of (6) and (7) for each band j:

bioRxiv preprint doi: https://doi.org/10.1101/2022.12.08.519675; this version posted December 9, 2022. The copyright holder for this preprint (which was not certified by peer review) is the author/funder, who has granted bioRxiv a license to display the preprint in perpetuity. It is made available under aCC-BY 4.0 International license.

$$sim_{ij} = \frac{S_{B,ij}^{(k)} \cdot \hat{T}_j^{(k)}}{\left\| S_{B,ij}^{(k)} \right\| \left\| \hat{T}_j^{(k)} \right\|}. \quad (8)$$

and sum (8) across all bands j to obtain a sim_i^{tot} index which ranges between 0-5, where 0 is no similarity between topographies and 5 is an exact match:

$$sim_i^{tot} = \sum_j sim_{ij}. \quad (9)$$

Since in this study we were not interested in the effect of post-menstrual age (PMA), before fitting model (1) we first regressed T_i^{tot}, $S_{B,i}^{tot}$ and sim_i^{tot} on PMA (linear regression), essentially removing PMA effect from all the variables. $S_{B,i}^{tot}$ and sim_i^{tot} were then centred (removing the mean value) before fitting the model (1).

RESULTS

Somatosensory-evoked slow neuronal activity is widespread across the scalp, while fast activity engages local somatotopically specific areas

We first defined the spectro-spatial characteristics of somatosensory-evoked activity in preterm neonates. Tactile stimulation of hands and feet evoked wideband power increases across all channels with two distinct peaks within the slow-delta band (6.7 and 3.7 dB at 0.8 Hz for hands and feet) and alpha-beta band (6.3 and 4.6 dB at 13 Hz for hands and feet, Fig. 1b and 2b). The topographic distribution of these energy changes was frequency dependent. Significant energy changes at slower frequencies (< 20 Hz) were widespread across the scalp, while changes at faster frequencies were focussed over the somatotopically appropriate scalp regions (contralateral and midline central channels following hands and feet stimulation respectively; Fig. 1c and d and Fig. 2c and d). This effect is more noticeable following feet stimulation (Fig. 2d).

bioRxiv preprint doi: https://doi.org/10.1101/2022.12.08.519675; this version posted December 9, 2022. The copyright holder for this preprint (which was not certified by peer review) is the author/funder, who has granted bioRxiv a license to display the preprint in perpetuity. It is made available under aCC-BY 4.0 International license.

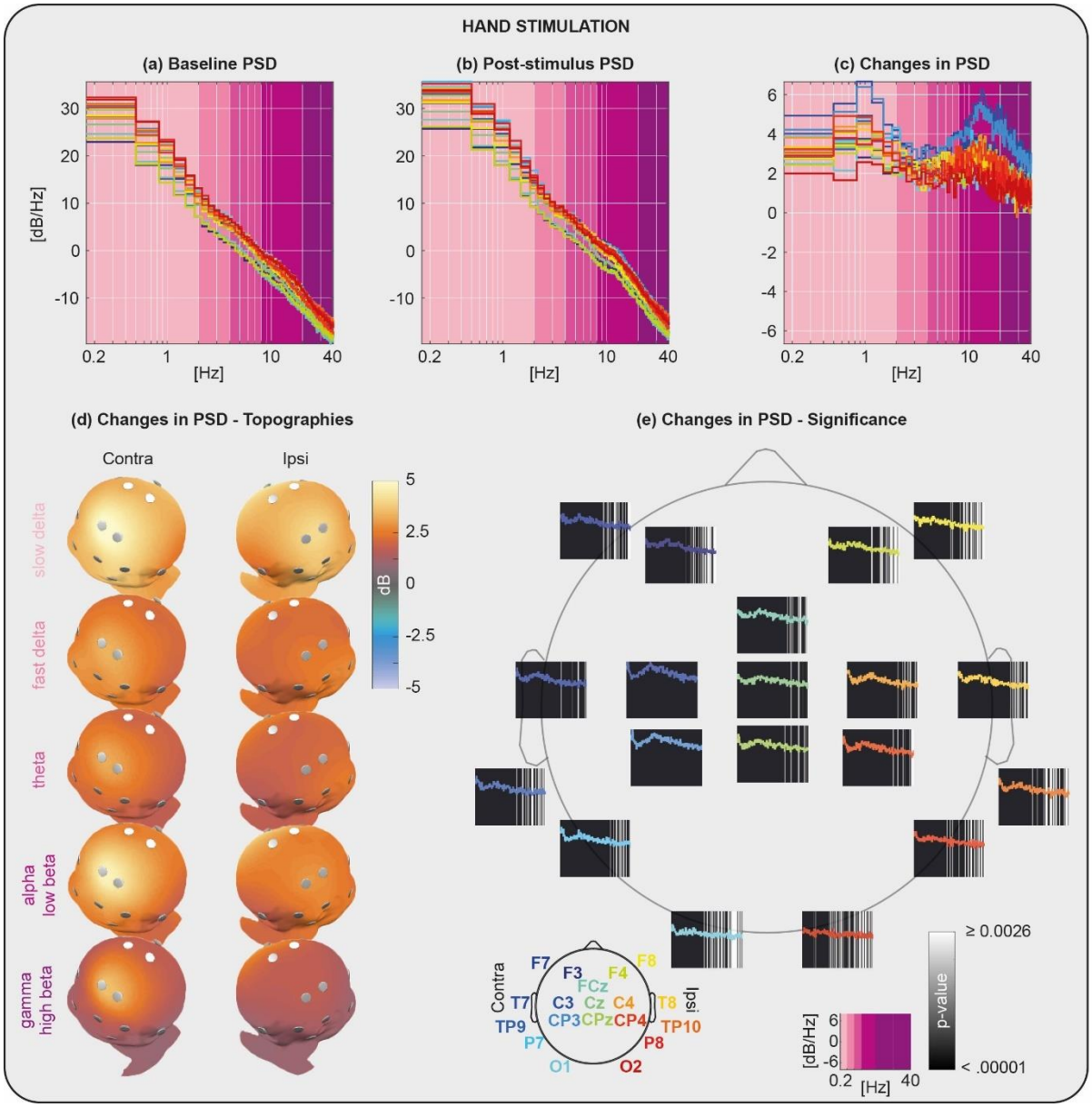

Figure 1. Spectro-spatial EEG power changes associated with tactile stimulation of the hands. Power spectral density (PSD) at baseline **(a)** and following stimulation **(b)** at each channel**.** PSD of changes elicited by the stimulation **(c)** and 3D maps of their scalp distribution in the slow-delta (0.2-2 Hz), fast-delta (2-4 Hz), theta (4-8 Hz), alpha-low beta (8-20 Hz) and high beta-gamma (20-40 Hz) band **(d)**. Statistical significance of the energy changes at each channel **(e)**, note that the changes are the same as those in panel (c) but on a linear frequency axis to allow resolution of faster frequencies.

bioRxiv preprint doi: https://doi.org/10.1101/2022.12.08.519675; this version posted December 9, 2022. The copyright holder for this preprint (which was not certified by peer review) is the author/funder, who has granted bioRxiv a license to display the preprint in perpetuity. It is made available under aCC-BY 4.0 International license.

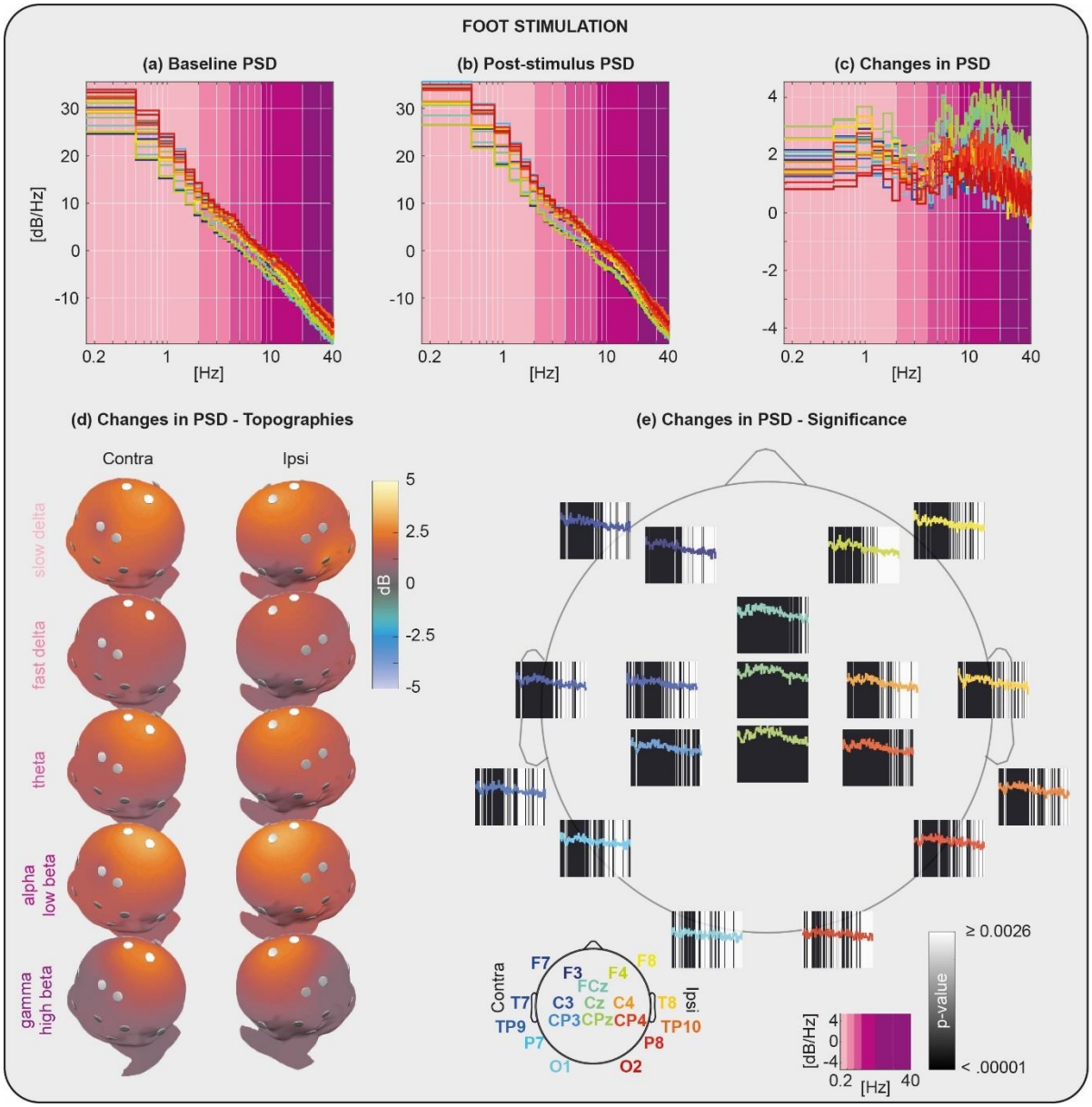

Figure 2. Spectro-spatial EEG power changes associated with tactile stimulation of the feet. Power spectral density (PSD) at baseline **(a)** and following stimulation **(b)** at each channel. PSD of changes elicited by the stimulation **(c)** and 3D maps of their scalp distribution in the slow-delta (0.2-2 Hz), fast-delta (2-4 Hz), theta (4-8 Hz), alpha-low beta (8-20 Hz) and high beta-gamma (20-40 Hz) band **(d)**. Statistical significance of the energy changes at each electrode **(e)**, note that the changes are the same as those in panel (c) but on a linear frequency axis to allow resolution of faster frequencies.

Endogenous activity influences EEG energy changes evoked by somatosensory stimulation

We then investigated how baseline energy with spectro-spatial characteristics similar to that of somatosensory-evoked activity affected the energy changes elicited with stimulation.

Energy changes evoked by tactile stimulation of hands and feet were strongly affected by the spontaneous activity preceding the stimulus (the linear model $T_i^{tot} = \beta_0 + \beta_1 S_{B,i}^{tot} + \beta_2 sim_i^{tot} + \beta_{12}(S_{B,i}^{tot} * sim_i^{tot})$ performed better in explaining the variance in T_i^{tot} than a constant model (hands: $r^2 = 0.55$, f-stats vs constant model = 286, $p < 0.0001$; feet: $r^2 = 0.46$, f-stats vs constant model = 226, $p < 0.0001$; Fig. 3a and 4a)).

bioRxiv preprint doi: https://doi.org/10.1101/2022.12.08.519675; this version posted December 9, 2022. The copyright holder for this preprint (which was not certified by peer review) is the author/funder, who has granted bioRxiv a license to display the preprint in perpetuity. It is made available under aCC-BY 4.0 International license.

Stimulus-evoked energy changes at average baseline energy and similarity were 13.17 dB (β_0 hands, t = 79.78, p < 0.0001) and 12.41 dB (β_0 feet, t = 77.41, p < 0.0001).
These stimulus-evoked energy changes decreased by 0.84 dB (β_1 hands, t = -26.8, p < 0.0001) and 0.71 dB (β_1 feet, t = -24.5, p < 0.0001) for every extra decibel of baseline energy (baseline energy main effect) at average similarity.
Also, higher *distribution similarity* was associated with smaller stimulus-evoked energy changes. Stimulus-evoked energy changes decreased by 4.87 dB (β_2 hands, t = -13.48, p < 0.0001) and 4.77 dB (β_2 feet, t = -9.26, p < 0.0001) for every extra degree of similarity at average baseline energy (similarity main effect).
Finally, the negative effect of baseline energy on stimulus-evoked energy changes was significantly stronger for higher degrees of similarity (β_{12} hands = -0.15, t = -2.71, p = 0.0068; β_{12} feet = -0.16, t = -2.01, p = 0.0450, Fig. 3a and 4a). This meant that energy changes decreased by 0.99 dB (hands) and 0.83 dB (feet) for every extra decibel of baseline energy at maximal similarity, but only by 0.55 dB (hands) and 0.50 dB (feet) at minimal similarity. The evoked somatotopic activity (i.e. at central contralateral central region for hand and midline central region for foot) preceded by high baseline energy with a spectro-spatial distribution similar to sensory-evoked activity were visually smaller than those preceded by low baseline energy with dissimilar distributions (Fig. 3d and 4d, for illustrative purposes).

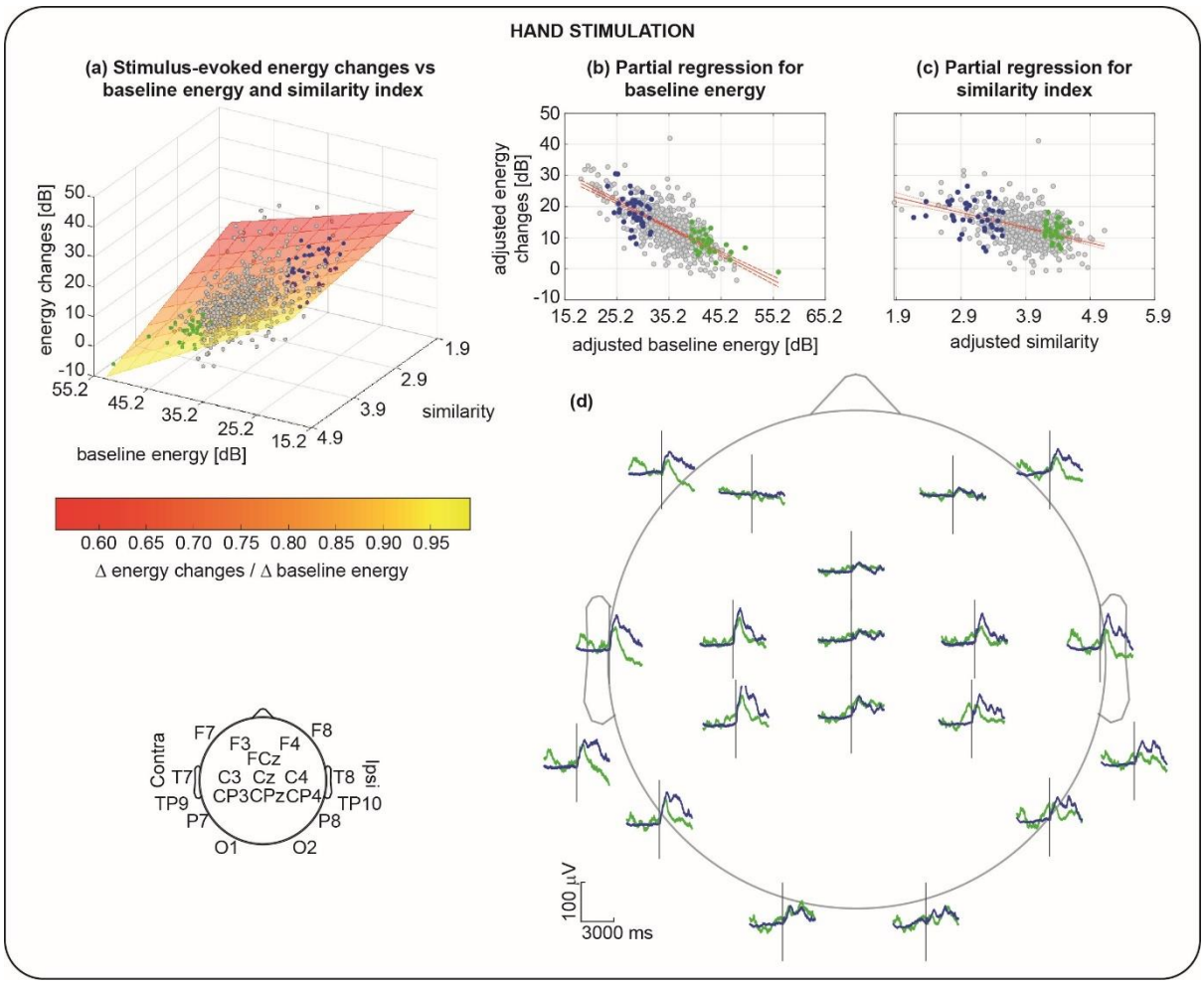

Figure 3. Endogenous activity influences EEG energy changes evoked by hands stimulation. Scatter plots of: **(a)** evoked energy changes (T^{tot}) vs baseline energy (S_B^{tot}) and spectro-spatial distribution similarity to sensory-evoked activity (sim^{tot}). The plane is the linear least square regression fit to data points (i.e. the graphical representation of the linear model $T_i^{tot} = \beta_0 + \beta_1 S_{B,i}^{tot} + \beta_2 sim_i^{tot} + \beta_{12}(S_{B,i}^{tot} * sim_i^{tot})$). Because of the significant interaction term β_{12}, the effect of baseline energy on

bioRxiv preprint doi: https://doi.org/10.1101/2022.12.08.519675; this version posted December 9, 2022. The copyright holder for this preprint (which was not certified by peer review) is the author/funder, who has granted bioRxiv a license to display the preprint in perpetuity. It is made available under aCC-BY 4.0 International license.

sensory-evoked energy changes (i.e. slope of the plane) depends on the level of similarity of the baseline spectro-spatial characteristics to that of somatosensory-evoked activity. The colorscale represents the slope of the plane at different levels of similarity; **(b)** evoked energy changes vs baseline energy after removing variance associated with sim^{tot} and $S_B^{tot} * sim^{tot}$. The solid red line is the partial regression leverage fit to data points (dashed red lines are the 95% confidence bounds of the fitted line); and **(c)** evoked EEG energy changes vs sim^{tot} after removing variance associated with S_B^{tot} and $S_B^{tot} * sim^{tot}$. The red line is the partial regression leverage fit to data points (dashed red lines are the 95% confidence bounds of the fitted line). In all panels each data point represents a single trial. Panel **(d)** shows the average of the scalp EEG recordings for the data points marked in green (top 25% $S_B^{tot} \cap$ top 25% sim^{tot}) and for those marked in blue (lowest 25% $S_B^{tot} \cap$ lowest 25% sim^{tot}).

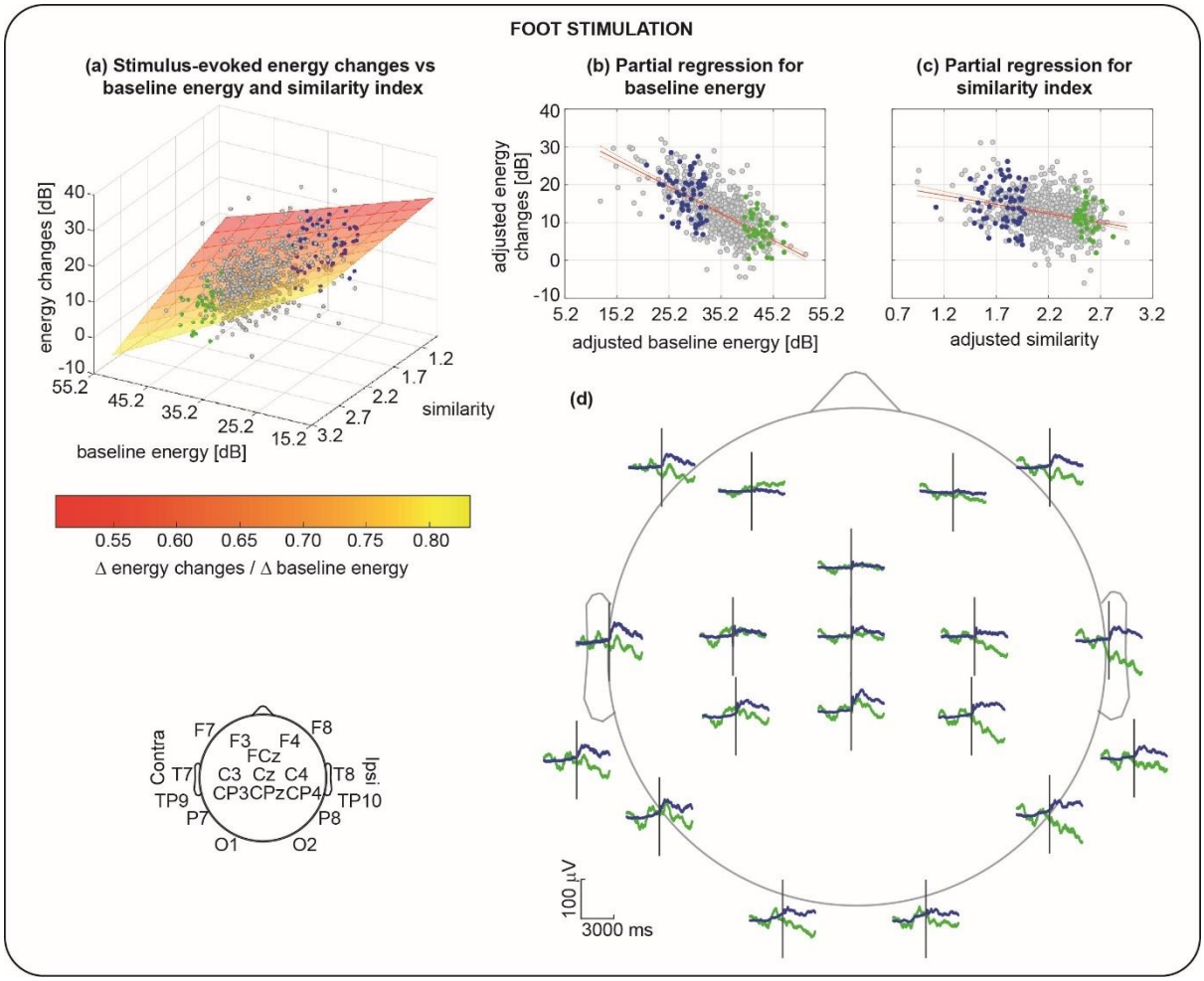

Figure 4. Endogenous activity influences EEG energy changes evoked by feet stimulation. Scatter plots of: **(a)** evoked energy changes (T^{tot}) vs baseline energy (S_B^{tot}) and spectro-spatial distribution similarity to sensory-evoked activity (sim^{tot}). The plane is the linear least square regression fit to data points (i.e. the graphical representation of the linear model $T_i^{tot} = \beta_0 + \beta_1 S_{B,i}^{tot} + \beta_2 sim_i^{tot} + \beta_{12}(S_{B,i}^{tot} * sim_i^{tot})$). Because of the significant interaction term β_{12}, the effect of baseline energy on sensory-evoked energy changes (i.e. slope of the plane) depends on the level of similarity of the baseline spectro-spatial characteristics to that of somatosensory-evoked activity. The colorscale represents the slope of the plane at different levels of similarity; **(b)** evoked energy changes vs baseline energy after removing variance associated with sim^{tot} and $S_B^{tot} * sim^{tot}$. The solid red line is the partial regression leverage fit to data points (dashed red lines are the 95% confidence bounds of the fitted line); and **(c)** evoked EEG energy changes vs similarity after removing variance associated with S_B^{tot} and $S_B^{tot} * sim^{tot}$. The red line is the partial regression leverage fit to data points (dashed red lines are the 95% confidence bounds of the fitted line). In all panels each data point represents a single

bioRxiv preprint doi: https://doi.org/10.1101/2022.12.08.519675; this version posted December 9, 2022. The copyright holder for this preprint (which was not certified by peer review) is the author/funder, who has granted bioRxiv a license to display the preprint in perpetuity. It is made available under aCC-BY 4.0 International license.

trial. Panel **(d)** shows the average of the scalp EEG recordings for the data points marked in green (top 25% $S_B^{tot} \cap$ top 25% sim^{tot}) and for those marked in blue (lowest 25% $S_B^{tot} \cap$ lowest 25% sim^{tot}).

Discussion

We demonstrated that spontaneous cortical activity with spectro-spatial distribution similar to that of somatosensory-evoked activity dampened energy changes elicited with stimulation. This suggests that endogenous activation of focal and extended somatosensory networks depresses their excitability in preterm human neonates. Tactile stimulation elicited an increase in EEG energy, but the extent of this increase was dependent on the spectro-spatial characteristics of the activity preceding the stimulus: the closer the spectro-spatial baseline cortical activity was to that evoked by the somatosensory stimulus, the weaker was the change elicited. This result offers the first etiological explanation to the discontinuous pattern of cortical activity at this age (burst-quiescence), which may be due to network refractoriness that recovers during inter-burst intervals (Vyazovskiy et al., 2009).

Tactile stimulation evokes focal and extended cortical activity changes in preterm neonates

External tactile (Leikos et al., 2020; Milh et al., 2007; Vanhatalo et al., 2009; Whitehead et al., 2018), noxious (Fabrizi et al., 2011; Green et al., 2018), visual (Colonnese et al., 2010) and auditory (Chipaux et al., 2013; Kaminska et al., 2018) stimuli elicit rudimentary cortical responses from as early as 28 weeks gestation in humans. These responses are generally composed of fast ripples overriding a larger slow wave focussed around the scalp locations overlaying the primary sensory areas relevant to stimulus modality (i.e. central – tactile; occipital – visual). Here we show that these responses (to tactile stimuli) have complex spectro-spatial characteristics, where oscillations at different frequencies have different voltage fields. The tactile response had a wide band power spectrum but included two clear peaks within the alpha-beta-gamma and slow-delta range and a dip in the theta range. Such coupled oscillatory signatures are a hallmark of activity-dependent processes at time scales relevant for synaptic plasticity (Buzsáki et al., 2013). Changes above 20 Hz (in the beta-gamma range) were localised to central contralateral and midline areas following hand and foot stimulation respectively, while those at the slow end of the spectrum were widespread.
Somatosensory stimulation elicits distinct patterns of oscillations which differentially synchronise neonatal cortical networks in rodent pups (Yang et al., 2009). Early Gamma Oscillations (EGO) involve focal networks limited to a single cortical column or barrel (McVea et al., 2012; Minlebaev et al., 2011; Yang et al., 2013), while long oscillations extend beyond those boundaries (Yang et al., 2009). EGO are driven by thalamic oscillators and are thought to support the development of thalamocortical projections and drive the organization of vertical topographic functional units (Minlebaev et al., 2011), while long oscillations may serve as a tangential signal binding these units together within the contralateral somatomotor area (An et al., 2014; Quairiaux et al., 2011; Yang et al., 2009). Further evidence of these oscillatory bands' distinct roles in somatosensory processing is that slow and fast evoked activity can be uncoupled by delivering proprioceptive-only or tactile-only stimuli in neonatal rats (Marcano-Reik and Blumberg, 2008).These oscillatory bands are also linked to the maturation of distinct neurotransmitter receptors (AMPA, NMDA and Kainate) (Minlebaev et al., 2009). As thalamo-cortical connections' formation precedes that of cortico-cortical connections in the human brain (Volpe, 2009), a role for slow oscillations in synchronising cortico-cortical ensembles may underlie why sensory-evoked delta activity declines later in preterm infants than fast ripples (Chipaux et al., 2013; Whitehead et al., 2018). Given that somatosensory stimulation of the hand evokes an hemodynamic response localised to the contralateral somatomotor area of the cortex in human preterm infants (Allievi et al., 2016), our results suggest that sensory evoked gamma activity may represent the focal activation of columnar functional sensory units, while slow activity may represent horizontal coordination between them within the contralateral somatomotor area.

bioRxiv preprint doi: https://doi.org/10.1101/2022.12.08.519675; this version posted December 9, 2022. The copyright holder for this preprint (which was not certified by peer review) is the author/funder, who has granted bioRxiv a license to display the preprint in perpetuity. It is made available under aCC-BY 4.0 International license.

Spontaneous engagement of somatosensory network suppresses their externally-driven excitability

Cortical bursts in preterm neonates can be evoked by sensory stimulation, but can also occur spontaneously in the absence of external stimuli (Whitehead et al., 2016) (Supplementary Video 2). These spontaneous activities occur with varying spatial configurations (Arichi et al., 2017) which overlap with those evoked by external stimulation (Bourel-Ponchel et al., 2021; Wallois et al., 2021; Whitehead et al., 2016). Here we show that the response to a somatosensory input is suppressed if the background cortical activity preceding the stimulus onset closely resembles that evoked by the stimulus itself.

In neonatal animal models, spontaneous activity starts from central pattern generators in the sensory periphery, spinal cord, thalamus or subplate (Martini et al., 2021). Independently of their source, these patterns ultimately involve the same cortical regions which are engaged by external stimuli and are confined within the domain related to one sensory modality (e.g. somatosensory: (Mizuno et al., 2018; Nakazawa et al., 2020); visual (Kenet et al., 2003; O'Hashi et al., 2018; Ruthazer and Stryker, 1996; Smith et al., 2018)). In human preterm neonates, resting-state fMRI activity involves the same areas engaged by sensory stimulation suggesting that these same networks can also be coherently active in the absence of any external stimulus (Allievi et al., 2016; Doria et al., 2010). As specific patterns of cortical activation correspond to specific patterns of voltage field distribution over the scalp (Arichi et al., 2017), background EEG with spectro-spatial characteristics similar to that evoked by somatosensory stimulation is likely to represent the spontaneous unsolicited activation of developing somatosensory networks.

Whether spontaneous or evoked, early activity patterns are supported by a mutually excitatory loop which comprises subplate neurons: a transient neuronal population in the immature brain, projecting to and receiving glutamatergic input from layers 4-6 of the cortical plate (Tolner et al., 2012; Viswanathan et al., 2012). Such a recurrent excitatory circuit will encounter activity-dependent synaptic depression, possibly because of transmitter depletion and ligand-induced changes in postsynaptic currents (Fedirchuk et al., 1999; Tabak et al., 2000) transiently reducing network excitability, which slowly recovers allowing for the next neuronal event, whether spontaneous or evoked, to occur. Our results therefore suggest that the spontaneous activation of somatosensory networks in preterm human neonates has a major dampening impact on the processing of later ascending sensory input.

In conclusion, we offer evidence that sensory-evoked activity in preterm human neonates represents the coordinated activation of local (columnar) and extended (tangential) cortical aggregates and that the occurrence of spontaneous cortical events in the same regions depresses their excitability preventing their immediate re-engagement. This "refractoriness" offers an etiological explanation to the cyclical burst-quiescence pattern typical of preterm cortical activity.

Acknowledgements

This work was supported by the Medical Research Council UK (MR/L019248/1 and MR/S003207/1) (awardee: LF), and Brain Research UK (awardee: KW). We would like to thank the families who participated in this research.

Supplementary Material

Supplementary Video 1: Example of tactile stimulation of the left hand in a 35 weeks post-menstrual age infant, during natural sleep. To maintain the infant's comfort, they remain wrapped in their bedding, with only a small amount of skin uncovered to deliver the tap.

bioRxiv preprint doi: https://doi.org/10.1101/2022.12.08.519675; this version posted December 9, 2022. The copyright holder for this preprint (which was not certified by peer review) is the author/funder, who has granted bioRxiv a license to display the preprint in perpetuity. It is made available under aCC-BY 4.0 International license.

Supplementary Video 2: Example of a spontaneous cortical burst in a 31 weeks post-menstrual age infant, during natural sleep.

Bibliography

Allievi, A.G., Arichi, T., Tusor, N., Kimpton, J., Arulkumaran, S., Counsell, S.J., Edwards, A.D., Burdet, E., 2016. Cerebral Cortex 26, 402–413.

An, S., Kilb, W., Luhmann, H.J., 2014. J. Neurosci. 34, 10870–10883.

André, M., Lamblin, M.-D., d'Allest, A.M., Curzi-Dascalova, L., Moussalli-Salefranque, F., Nguyen The Tich, S., Vecchierini-Blineau, M.-F., Wallois, F., Walls-Esquivel, E., Plouin, P., 2010. Neurophysiologie Clinique/Clinical Neurophysiology 40, 59–124.

Arichi, T., Whitehead, K., Barone, G., Pressler, R., Padormo, F., Edwards, A.D., Fabrizi, L., 2017. eLife 6, e27814.

Bourel-Ponchel, E., Gueden, S., Hasaerts, D., Héberlé, C., Malfilâtre, G., Mony, L., Vignolo-Diard, P., Lamblin, M.-D., 2021. Neurophysiologie Clinique 51, 61–88.

Buzsáki, G., Logothetis, N., Singer, W., 2013. Neuron 80, 751–764.

Chipaux, M., Colonnese, M.T., Mauguen, A., Fellous, L., Mokhtari, M., Lezcano, O., Milh, M., Dulac, O., Chiron, C., Khazipov, R., Kaminska, A., 2013. PLOS ONE 8, e79028.

Colonnese, M.T., Kaminska, A., Minlebaev, M., Milh, M., Bloem, B., Lescure, S., Moriette, G., Chiron, C., Ben-Ari, Y., Khazipov, R., 2010. Neuron 67, 480–498.

Doria, V., Beckmann, C.F., Arichi, T., Merchant, N., Groppo, M., Turkheimer, F.E., Counsell, S.J., Murgasova, M., Aljabar, P., Nunes, R.G., Larkman, D.J., Rees, G., Edwards, A.D., 2010. PNAS 107, 20015–20020.

Fabrizi, L., Slater, R., Worley, A., Meek, J., Boyd, S., Olhede, S., Fitzgerald, M., 2011. Current Biology 21, 1552–1558.

Fabrizi, L., Verriotis, M., Williams, G., Lee, A., Meek, J., Olhede, S., Fitzgerald, M., 2016. Sci Rep 6.

Fedirchuk, B., Wenner, P., Whelan, P.J., Ho, S., Tabak, J., O'Donovan, M.J., 1999. J. Neurosci. 19, 2102–2112.

Feller, M.B., Wellis, D.P., Stellwagen, D., Werblin, F.S., Shatz, C.J., 1996. Science 272, 1182–1187.

Godfrey, K.B., Swindale, N.V., 2007. PLOS Computational Biology 3, e245.

Green, G., Hartley, C., Hoskin, A., Duff, E., Shriver, A., Wilkinson, D., Adams, E., Rogers, R., Moultrie, F., Slater, R., 2018. PAIN Articles in Press.

Guérit, J.-M., Amantini, A., Amodio, P., Andersen, K.V., Butler, S., de Weerd, A., Facco, E., Fischer, C., Hantson, P., Jäntti, V., Lamblin, M.-D., Litscher, G., Péréon, Y., 2009. Neurophysiologie Clinique/Clinical Neurophysiology 39, 71–83.

Kaminska, A., Delattre, V., Laschet, J., Dubois, J., Labidurie, M., Duval, A., Manresa, A., Magny, J.-F., Hovhannisyan, S., Mokhtari, M., Ouss, L., Boissel, A., Hertz-Pannier, L., Sintsov, M., Minlebaev, M., Khazipov, R., Chiron, C., 2018. Cereb Cortex 28, 3429–3444.

Kenet, T., Bibitchkov, D., Tsodyks, M., Grinvald, A., Arieli, A., 2003. Nature 425, 954–956.

Khazipov, R., Luhmann, H.J., 2006. Trends in Neurosciences, Nature and nurture in brain development and neurological disorders 29, 414–418.

Leikos, S., Tokariev, A., Koolen, N., Nevalainen, P., Vanhatalo, S., 2020. European Journal of Neuroscience 51, 1059–1073.

Marcano-Reik, A.J., Blumberg, M.S., 2008. European Journal of Neuroscience 28, 1457–1466.

Martini, F.J., Guillamón-Vivancos, T., Moreno-Juan, V., Valdeolmillos, M., López-Bendito, G., 2021. Neuron 109, 2519–2534.

McVea, D.A., Mohajerani, M.H., Murphy, T.H., 2012. J. Neurosci. 32, 10982–10994.

Milh, M., Kaminska, A., Huon, C., Lapillonne, A., Ben-Ari, Y., Khazipov, R., 2007. Cerebral Cortex 17, 1582–1594.

Minlebaev, M., Ben-Ari, Y., Khazipov, R., 2009. Cereb Cortex 19, 688–696.

bioRxiv preprint doi: https://doi.org/10.1101/2022.12.08.519675; this version posted December 9, 2022. The copyright holder for this preprint (which was not certified by peer review) is the author/funder, who has granted bioRxiv a license to display the preprint in perpetuity. It is made available under aCC-BY 4.0 International license.

Minlebaev, M., Colonnese, M., Tsintsadze, T., Sirota, A., Khazipov, R., 2011. Science.
Mizuno, H., Ikezoe, K., Nakazawa, S., Sato, T., Kitamura, K., Iwasato, T., 2018. Cell Reports 22, 123–135.
Molnár, Z., Luhmann, H.J., Kanold, P.O., 2020. Science 370.
Nakazawa, S., Yoshimura, Y., Takagi, M., Mizuno, H., Iwasato, T., 2020. J. Neurosci. 40, 7637–7650.
O'Donovan, M.J., 1999. Current Opinion in Neurobiology 9, 94–104.
O'Hashi, K., Fekete, T., Deneux, T., Hildesheim, R., van Leeuwen, C., Grinvald, A., 2018. Cerebral Cortex 28, 1794–1807.
Quairiaux, C., Megevand, P., Kiss, J.Z., Michel, C.M., 2011. Journal of Neuroscience 31, 9574–9584.
Ruthazer, E.S., Stryker, M.P., 1996. J. Neurosci. 16, 7253–7269.
Saby, J.N., Meltzoff, A.N., Marshall, P.J., 2016. International Journal of Psychophysiology 110, 146–152.
Smith, G.B., Hein, B., Whitney, D.E., Fitzpatrick, D., Kaschube, M., 2018. Nat Neurosci 21, 1600–1608.
Tabak, J., Senn, W., O'Donovan, M.J., Rinzel, J., 2000. J. Neurosci. 20, 3041–3056.
Tiriac, A., Del Rio-Bermudez, C., Blumberg, M.S., 2014. Current Biology 24, 2136–2141.
Tolner, E.A., Sheikh, A., Yukin, A.Y., Kaila, K., Kanold, P.O., 2012. J. Neurosci. 32, 692–702.
Tsuchida, T.N., Wusthoff, C.J., Shellhaas, R.A., Abend, N.S., Hahn, C.D., Sullivan, J.E., Nguyen, S., Weinstein, S., Scher, M.S., Riviello, J.J., Clancy, R.R., American Clinical Neurophysiology Society Critical Care Monitoring Committee, 2013. J Clin Neurophysiol 30, 161–173.
Vanhatalo, S., Jousmäki, V., Andersson, S., Metsäranta, M., 2009. Pediatr Res 66, 710–713.
Viswanathan, S., Bandyopadhyay, S., Kao, J.P.Y., Kanold, P.O., 2012. J. Neurosci. 32, 1589–1601.
Volpe, J.J., 2009. Seminars in Pediatric Neurology 16, 167–178.
Vyazovskiy, V.V., Faraguna, U., Cirelli, C., Tononi, G., 2009. Journal of Neurophysiology 101, 1921–1931.
Wallois, F., Routier, L., Heberlé, C., Mahmoudzadeh, M., Bourel-Ponchel, E., Moghimi, S., 2021. Neurophysiologie Clinique 51, 5–33.
Watanabe, K., Hayakawa, F., Okumura, A., 1999. Brain and Development 21, 361–372.
Whitehead, K., Meek, J., Fabrizi, L., 2018. Scientific Reports 8, 17516.
Whitehead, K., Pressler, R., Fabrizi, L., 2016. Clinical Neurophysiology Practice 2, 12–18.
Worley, A., Fabrizi, L., Boyd, S., Slater, R., 2012. Journal of Neuroscience Methods 205, 252–257.
Yang, J.-W., An, S., Sun, J.-J., Reyes-Puerta, V., Kindler, J., Berger, T., Kilb, W., Luhmann, H.J., 2013. Cerebral Cortex 23, 1299–1316.
Yang, J.-W., Hanganu-Opatz, I.L., Sun, J.-J., Luhmann, H.J., 2009. J. Neurosci. 29, 9011–9025.
Zheng, J., Lee, S., Zhou, Z.J., 2006. Nat Neurosci 9, 363–371.